Comparative Analysis of Field and Simulation Experiments on an Asynchronous Motor

K. Wilkosz, M. Sobierajski
Wroclaw University of Technology,
Wroclaw, Poland
wilk@see.ie.pwr.wroc.pl

W. T. Kwasnicki, M. Reformat
Manitoba HVDC Research Centre,
Winnipeg, Canada
wk@hvdc.ca

Abstract - **A comparative analysis of field and simulation experiments on an asynchronous motor is presented. Factors affecting the modelling accuracy of the asynchronous motor are discussed. Conditions at which the simulation test and measurement results were in the closest agreement are outlined.**

Keywords: Asynchronous Motor, Electromagnetic Transients, Simulation Model.

I. INTRODUCTION

Often, in order to solve a given electrical problem, it is hard to perform the necessary experiments on a real system. Such experiments are usually difficult, expensive and can endanger power system security. On the other hand, the simulation experiments are cheaper, they are easier and safer to conduct, and they do not affect the real system operation at all. Providing that the model is adequate, all the experimentation work can be done on a computer and only the confirmation tests performed on a real system.

In this paper, an experiment conducted on a motor operating in the industrial power network at the Copper Smelting Works in Glogow, Poland is described. At the same time, results of simulation experiments on a computer model of the same part of the power network are presented. These simulation experiments have been performed to examine the modelling accuracy.

The main objective of this paper is to present a comparative analysis of the real system measurements and the simulation test results for the asynchronous motor supplied from the industrial power network. For the simulation tests PSCAD/EMTDC electromagnetic transients simulation program has been used and the motor model included in the software was adapted for the experiments.

II. FIELD EXPERIMENT

A. Test System

A 6kV, 500kW asynchronous motor operated at the Copper Smelting Works in Glogow, Poland is considered. The electric circuit, shown in Fig. 1, consists of two substations: S1 and S2 connected by a cable C2 and a current-limiting reactor. Another cable C1 is also connected to substation S1. At the end of this cable a three-phase line-to-ground fault is applied. The asynchronous motor and a 6.0/0.4kV, 1MVA transformer are connected to substation S2. A group of low voltage motors is also connected to the 0.4 kV side of the substation S2 transformer. The system supplying the industrial power network is connected to the 110 kV side of the substation S1 transformer.

B. Experiments

Experiments were aimed at observing the motor operating after sudden drop of voltage at the bus supplying the motor. During these experiments an instantaneous phase voltage at bus S2 V_{S2a} was recorded along with a reference voltage V_r observed at the bus of another substation separated from buses S1 and S2. The difference between the voltages V_{S2a} and V_r was also recorded. (Fig. 2, 3). The experiments were performed during the following circuit conditions:

a) a 3-phase line-to-ground fault is applied at the end of the cable C1 not connected to bus S1
b) the cable C1 is connected by closing the switch W1
c) the cable C2 is disconnected by opening the switch W2 approximately 0.2 s after closing the switch W1.

III. SIMULATION EXPERIMENT

A. System Model

For the circuit considered in the field experiments shown in Fig. 1, a simulation 3-phase model was built using the PSCAD/EMTDC electromagnetic transient simulation program.

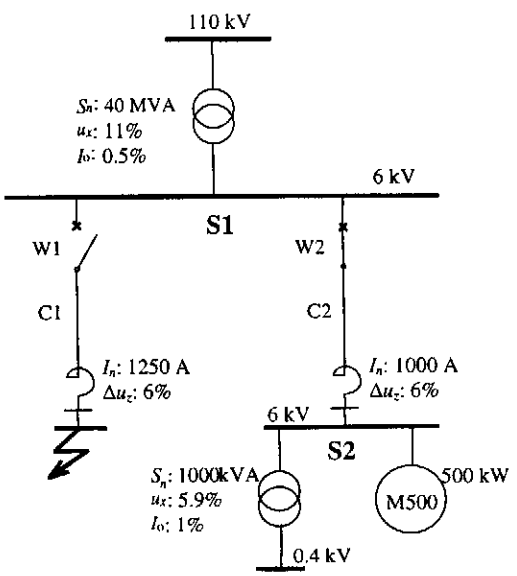

Fig. 1. Part of the system considered for experiments.

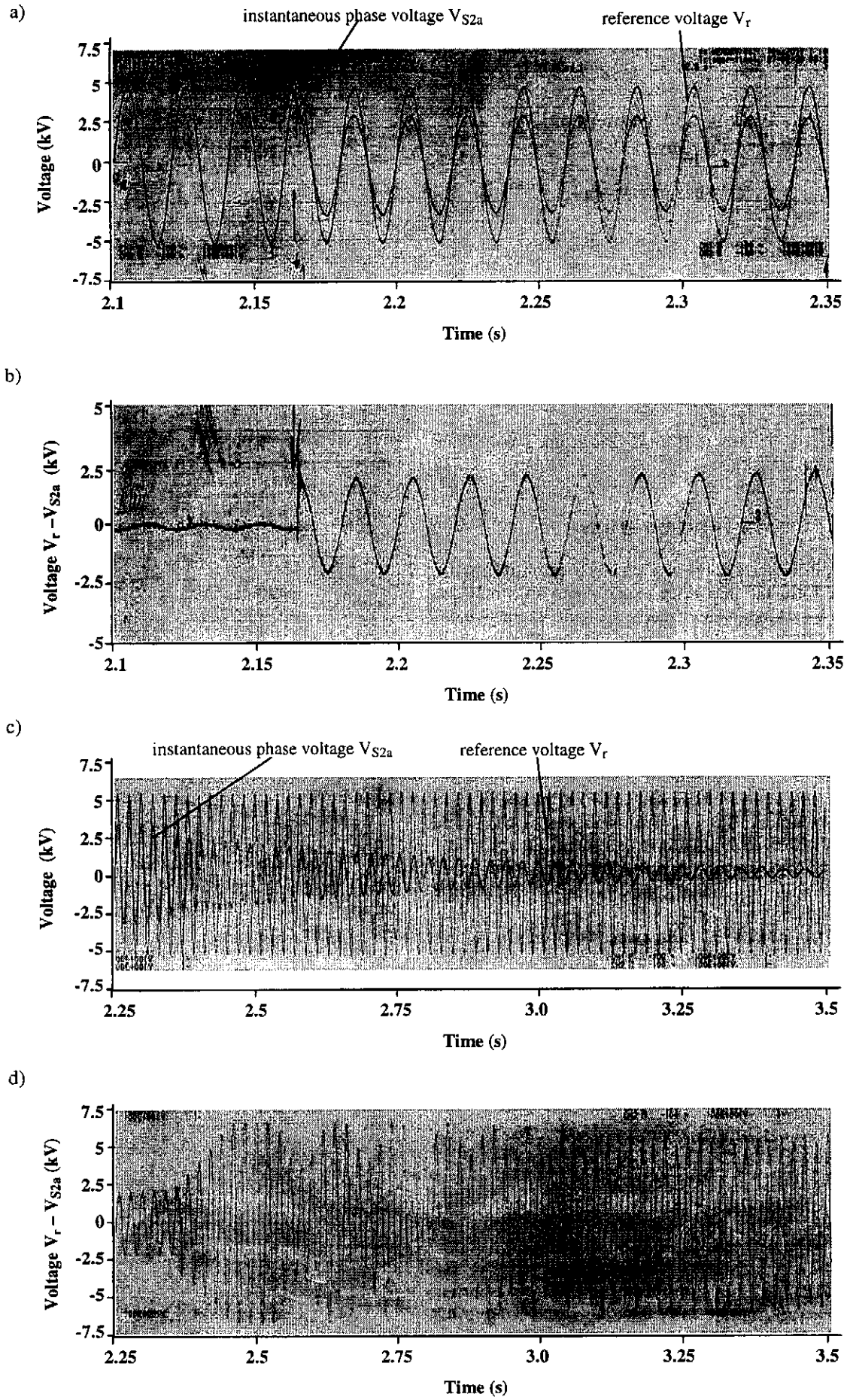

Fig. 2. Results of field experiments: a), b) before opening W2; c), d) immediately before and after opening W2.

a)

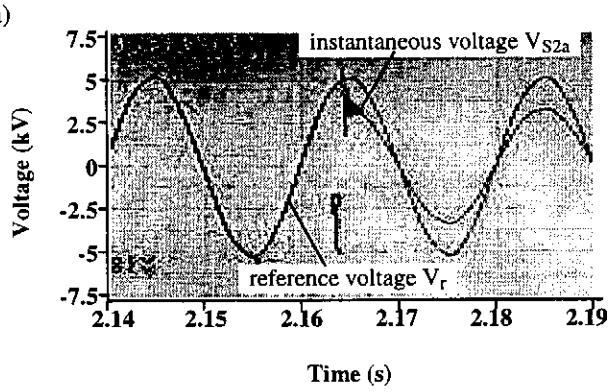

b)

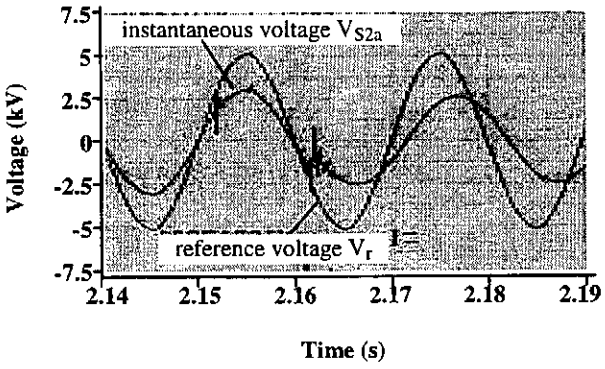

Fig. 3. Voltage V_{S2a} during simulation at: a) closing W1, b) opening W2.

The system supplying the substation S1 was represented by a Thevenin equivalent placed on the 110kV side of substation transformer. The cables C1 and C2, present in the circuit, were modelled as Π–sections. To represent a group of low voltage motors a reactance was placed on the 0.4 kV side of the S2 substation transformer, which value was calculated to be equal to 0.204 Ω.

The simulation test reconstructed the sequence of events as it happened in the field experiment. The motor parameters were verified during simulation runs, which were performed with different integration time-steps.

B. Motor Model and its Parameters

A squirrel cage induction machine model (SQC100), included in the PSCAD/EMTDC program, was used for modelling the motor. This is a model of a double cage machine but only one cage was actually used. The equivalent circuit for the direct-axis of the generalized machine used by the PSCAD/EMTDC program is shown in Fig. 4. In this figure L_1 is a stator leakage inductance, L_M is a magnetizing inductance, L_2, L_3 are first and second cage inductance, L_{23} is a rotor mutual inductance, R_1 is a stator resistance, and R_2, R_3 are first and second cage resistances.

It was assumed that the mechanical torque in the motor model was a square function of the rotor angular speed. For the mechanical system of the motor running a pump, the polar moment of inertia J was initially set to 0.54 MWs/MVA.

Not all of the parameters required for the motor model were possible to obtain from the system data so that they had to be determined experimentally prior to the simulation

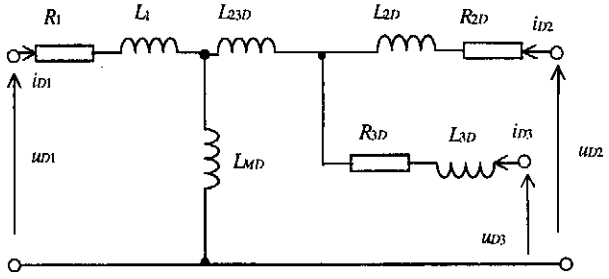

Fig. 4. Electrical machine direct-axis equivalent circuit used in PSCAD/EMTDC.

tests. The initial values were adopted from [2] and are shown in Table 1. Those parameters correspond to the transient electromechanical state model shown in Fig. 5. Based on these values, parameters of the equivalent circuit in Fig. 4 were initialized.

The initial values of the motor model parameters were then modified so that the rated active power and rated current were matched at steady-state. The calculations of elements of the equivalent circuit in Fig. 5 and then verification of those values with the PSCAD/EMTDC simulation runs, allowed to establish the final values of R_s, R_r, X_s, X_m, and X_r, also shown in Table 1.

Table 1. Initial & final values of the motor model parameters

Parameters	R_s p.u.	X_s p.u.	X_m p.u.	R_r p.u.	X_r p.u.
Initial values	0.013	0.067	3.8	0.0090	0.17
Final values	0.013	0.050	3.8	0.0036	0.17

The preliminary simulation experiments were aimed at reproducing the real system measurements and beside the verification of electrical parameters it was also found that the polar moment of inertia J should be equal to 0.5 MWs/MVA.

C. *Simulation Results*

The simulation results are presented in Fig. 6 and 7. Shown there is the instantaneous voltage at bus S2 V_{S2a} and its comparison to the reference voltage V_r.

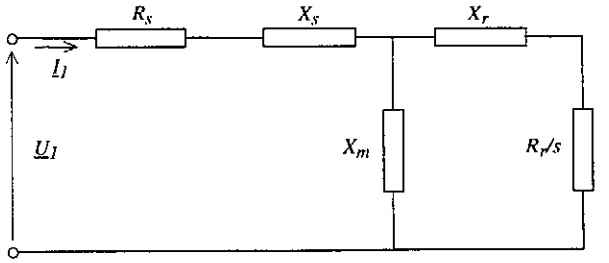

Fig. 5. Asynchronous motor equivalent circuit for transient electromechanical states.

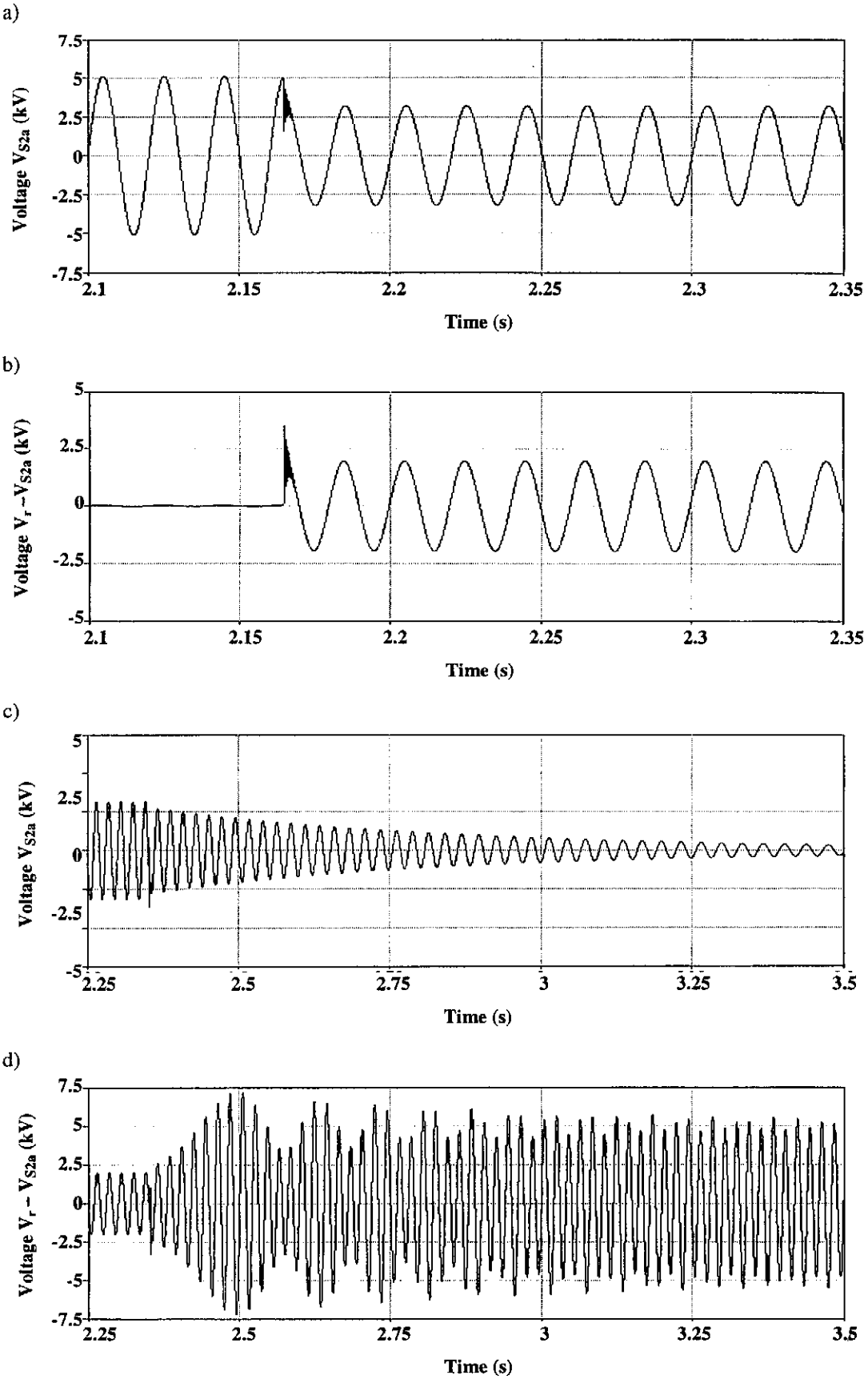

Fig. 6. Simulation results: a), c) instantaneous phase voltage V_{S2a}, b), d) difference of voltages V_r - V_{S2a}; $\tau_1 = 5$ µs.

a)

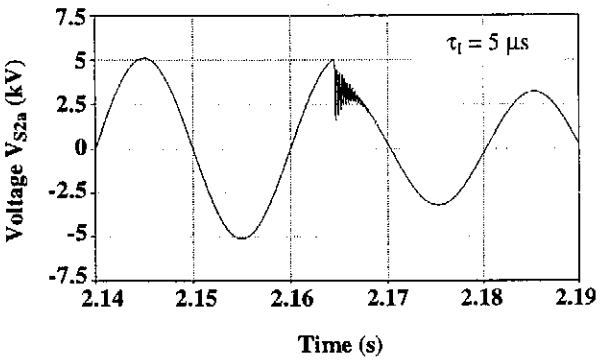

b)

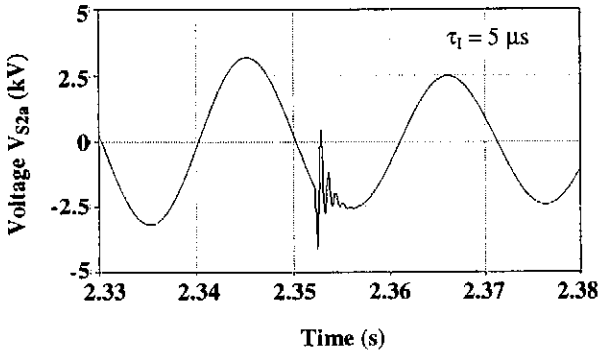

Fig. 7. Voltage V_{S2a} during simulation at:
a) closing W1, b) opening W2.

IV. FACTORS AFFECTING SIMULATION EXPERIMENTS

Simulation parameters, accuracy of system component models, and model interfacing to the network solution have significant influence on simulation process and its results. Some of the elements, which were found important for the simulation experiments, are described below.

A. *Integration Time-Step*

The effect of integration time-step on the simulation results was investigated. Simulation runs were performed with time-step values equal to 100μs, 50μs, 25μs and 5μs. Low frequency oscillations of the voltage V_{S2} were observed in all cases and were found to be in a close match with the field measurements (Fig. 2).

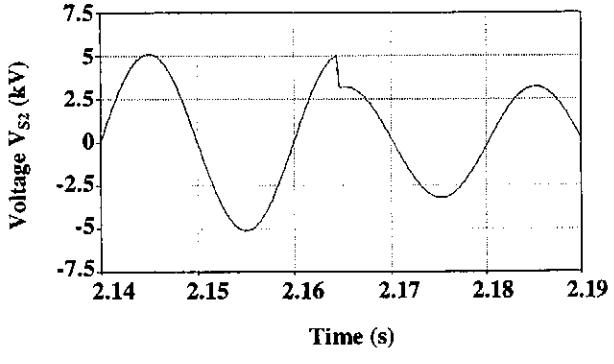

Fig. 8. Voltage V_{S2a} during simulation at closing W1 for τ_I = 25, 50, 100 μs.

The high frequency voltage oscillations after closing the switch W1, as seen in Fig. 3, were observed only for simulation time-step equal to 5μs, see Fig. 7a and Fig. 8. The high frequency oscillations after opening the switch W2 were observed in all cases shown in Fig. 7b and Fig. 9. A more thorough investigation of the high frequency voltage oscillations allowed identifying two reasons of they occurrence: resonance oscillations of the electrical circuit, and numerical oscillations due to large integration steps.

When small time-step was used (less than 50μs), the numerical oscillations after opening W2 diminished and the voltage waveforms were in close match with those observed in real system.

B. *Cable Model*

Cables in the system were represented by Π-sections. This approach allowed obtaining realistic low and high frequency oscillations of voltage V_{S2}. The same kind of voltage distortion was observed when the cable C2 was repre-

a)

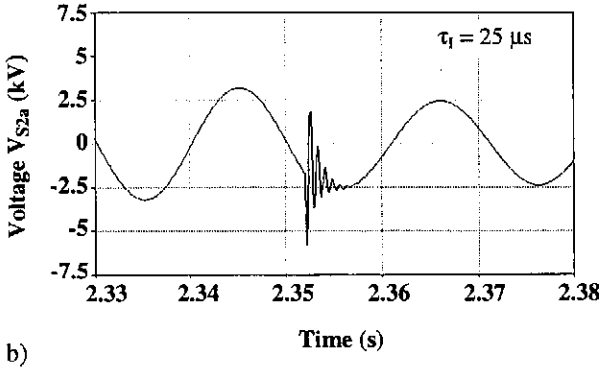

b)

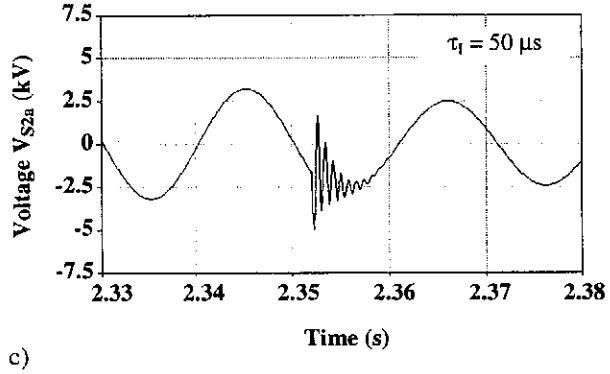

c)

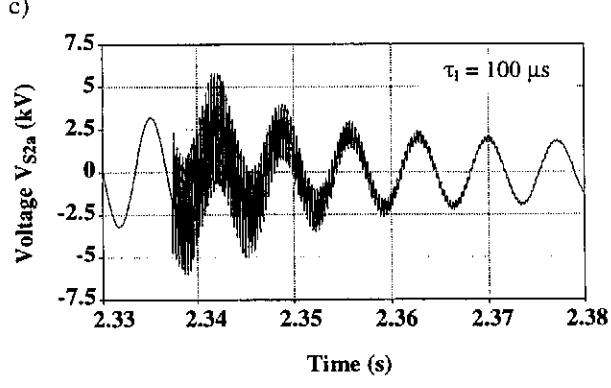

Fig. 9. Voltage V_{S2a} during simulation at switching W2 off.

sented using resistance and inductance along with lumped capacitance. An attempt to represent the cable only by resistance and inductance led to improper dynamic behaviour (lost of high frequency oscillations) and also to numerical problems. For small integration time-steps the problems appeared as voltage spikes seen in the voltage waveforms just after opening the switch W2. This problem was earlier reported and described in [1]. A discussion related to them is included in subsection IV. D.

C. Motor Parameters

Since not all of the data for motor model was available, an approach was undertaken to adapt the initial parameter values from the work described in [2]. The original set of parameter values was then modified so that the rated power and rated current of the motor at steady-state were matched. It was found that the most critical values were the R_3 (R_r), L_1 (X_s), and L_3 (X_r).

D. Interfacing Machine Model to Network

Machine model in time domain simulation program is represented as a current source [1]. Computation of the amount of current injection to the network is typically performed in a separate subroutine and it depends on the terminal voltage obtained from the network solution in the previous time-step.

In order to maintain computational stability when the machine operates near open circuit condition, a smaller time-step is required. Alternatively a small capacitance or large resistance from the machine terminals to ground can be placed to prevent the machine to be completely open circuited.

It was found that terminating the machine to the network could be satisfactory accomplished through its characteristic impedance as shown in Fig. 10 [1]. For the synchronous machine this characteristic impedance was chosen as the subtransient reactance and for the induction motor was chosen as the total leakage reactance.

If L_c is the characteristic inductance and Δt is the network solution time-step, the resistance R_c for the EMTDC network admittance matrix is computed by:

$$R_c = 2\,L_c/\Delta t\,. \tag{1}$$

In this case, instead of injecting the calculated machine current I_m, the current injected is given by:

$$I_{mach}(t) = I_m(t) + I_c(t), \tag{2}$$

where $I_c(t)$ is a compensating current calculated using the formula:

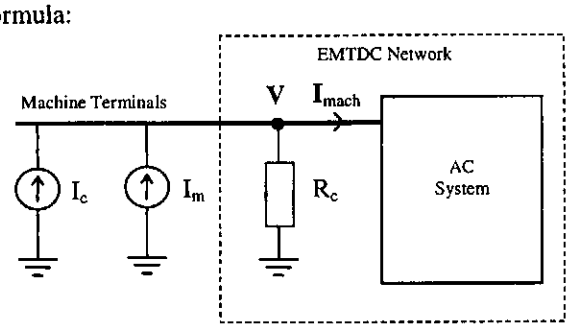

Fig. 10. Machine model interface.

$$I_c(t) = V(t - \Delta t)/R_c, \tag{3}$$

where $V(t - \Delta t)$ is the voltage in the previous time-step.

For a sudden voltage change, the compensated current $I_{mach}(t)$ is not calculated until the next time-step and its injection to an open circuit would cause spurious voltage spikes. The network sees, however, impedance R_c instead of an open circuit, which is exactly the instantaneous impedance the machine would be represented in the EMTDC main matrix.

Although this method improves the machine model behaviour, numerical problems may still take place for a sudden voltage change if the integration step is too small. In order to mitigate the problem, an additional shunt resistance or a shunt capacitance may be needed. In practical system models, however, such elements are naturally present in the electrical circuit. In our case, for example, the models of two cables connected to the motor terminals introduced sufficient capacitance to eliminate the voltage spikes.

V. CONCLUSIONS

The simulation results presented in the paper are found to be in a close match with the voltage waveforms from the field measurements. System dynamic behaviour after fault application and disconnecting motor terminals has been reproduced. Low and high frequency oscillations, similar to those observed in a real system, are present in the voltage waveforms. The level of match of the simulation results and the voltage waveforms from the field measurements is as follows: the amplitude of the voltage before opening W2: $\geq 98\%$, the amplitude of the voltage after opening W2: $\geq 92\%$, the amplitude of the high frequency voltage oscillations: $\geq 85\%$.

In order to simulate system dynamic behaviour in details, including high frequency oscillations, small simulation time-steps must be used. If the details are not required, larger time-steps can be used but numerical problems, associated with integration method may be encountered if this time-step is too large.

The studies indicated that an adjustment of model parameters during validation tests is hardly avoidable and it should be accounted as an integral part of the system modelling process.

VI. REFERENCES

[1] Gole A.M., Menzies R.W.,Turanli H.M., Woodford D.A., "Improved Interfacing of Electrical Machine Models to Electromagnetic Transients Programs", *IEEE transactions on Power Apparatus and Systems*, Vol. PAS-103, No 9, September 1984.

[2] Berg G., Kar A., "Model representation of power system loads", *Proceedings of PICA* 1971.

[3] Sobierajski M., Wilkosz K., "Computer simulation of transient behaviour of motors supplied by 6kV substation OSR22/1 in Copper Smelting Works, Glogow, Poland. The results", *Technical Report of Institute of Electrical Power Engineering*, Wrocław University of Technology, No. 19, 1998 (in Polish).